Quenching of Photoluminescence from Porous Silicon by Aromatic Molecules

Jae Hee Song and Michael J. Sailor*

Contribution from the Department of Chemistry and Biochemistry, The University of California at San Diego, La Jolla, California 92093-0358

Received April 16, 1997[⊗]

Abstract: A systematic study of the efficiency of photoluminescence (PL) quenching of nanocrystalline porous Si by aromatic triplet energy acceptors was carried out. The effects of molecular triplet energy, molecular size, and the porous Si emission energy on PL quenching efficiency were probed. Photoluminescent porous Si samples, prepared by electrochemical etch, were titrated with toluene solutions of anthracene, 9,10-diphenylanthracene, 9,10-dichloroanthracene, 9,10-dimethylanthracene, pyrene, 1,2-benzanthracene, acridine, and 1,4-diphenyl-1,3-butadiene, and the steady-state and time-resolved PL spectra were measured. The quenching of PL adequately fits a dynamic Stern−Volmer quenching model. The rate of quenching increases with increasing exoergicity, and then levels off at higher exoergicities. The mechanism of quenching is attributed to energy transfer from the porous Si excited state to the triplet levels of the quencher molecules. The rate of quenching can also be affected by the size of substituents on the quenchers; some molecules with larger substituents display slower quenching rates than expected from their triplet energies.

Introduction

The discovery of visible photo- and electroluminescence from nanocrystalline ("porous") silicon has created interest in the material for potential display[1−3] and chemical sensor applications.[4−14] An important feature of this material is that its photoluminescence properties can be controlled by interfacial electron-, hole-, and energy-transfer processes. For example, many organic aromatic molecules have been shown to efficiently quench photoluminescence from porous silicon.[7,15−17] Comparison of the quenching data with the oxidation potentials, reduction potentials, and triplet energy levels led to the conclusion that the quenching process for aromatic molecules is predominantly driven by energy transfer.[7] However, the rate of this energy transfer quenching as a function of driving force has not been quantified. Because the wavelength of the photoluminescence maximum of porous silicon can be readily tuned by adjusting the preparation conditions, the material provides a convenient means for studying the energy dependence of the quenching process. In this work, we have prepared different porous silicon samples whose emission wavelengths range between 500 and 800 nm and probe the efficiency of quenching as a function of the emission energy.

Experimental Section

Sample Preparation and Treatment. Luminescent porous Si samples were prepared by galvanostatic photoetch of polished crystalline n-Si (phosphorus doped, 0.58 Ω cm resistivity, (100) orientation) supplied by International Wafer Service. The etching solution was prepared by adding an equal volume of pure ethanol (Quantum Chemicals) to an aqueous solution of HF (48% by weight; Fisher Scientific). The etching cell was constructed of Teflon and was open to air. Si wafers were cut into squares with a diamond scribe and mounted in the bottom of the Teflon cell with a Viton O-ring seal, exposing 0.2 cm^2 of the Si surface. Electrical contact was made to the back side of the Si wafer with a strip of heavy Al foil. A loop of Pt wire was used as a counter electrode. Samples were illuminated during the etch with a 300 W tungsten lamp in order to supply a photocurrent for the corrosion reaction.[18] Etching was carried out differently depending upon the spectral emission maximum desired: type A samples were etched at an anodic current density of 10 mA/cm^2 for 60 min; type B samples were etched at an anodic current density of 5 mA/cm^2 for 30 min, followed by a 5 min etch at 50 mA/cm^2; type C samples were etched at an anodic current density of 3 mA/cm^2 for 30 min with half the photoetch light intensity used in types A and B; and type D samples were etched at an anodic current density of 3 mA/cm^2 for 30 min with $^1/_3$ the photoetch light intensity used in types A and B. After etching, the samples were rinsed in 95% ethanol, dried under a stream of dry $N_{2(g)}$, and then dried *in vacuo* for 30 min prior to use. From this point on, standard inert atmosphere (nitrogen) techniques were used to avoid introduction of air or water.[19]

Anthracene, 9,10-diphenylanthracene, 9,10-dimethylanthracene, pyrene, 1,2-benzanthracene, and 1,4-diphenyl-1,3-butadiene were obtained from Aldrich Chemical Co. 9,10-Diphenylanthracene and acridine were used as received from Acros. Stock solutions of the molecules were prepared from HPLC-grade toluene (Aldrich chemical Co.) which was freeze−

* Author to whom correspondence should be addressed.

⊗ Abstract published in *Advance ACS Abstracts,* July 15, 1997.

(1) Fauchet, P. M. *J. Lumin.* **1996**, *70*, 294−309.
(2) Hirschman, K. D.; Tsybeskov, L.; Duttagupta, S. P.; Fauchet, P. M. *Nature* **1996**, *384*, 338−341.
(3) Collins, R. T.; Fauchet, P. M.; Tischler, M. A. *Phys. Today* **1997**, *50*, 24−31.
(4) Lauerhaas, J. M.; Sailor, M. J. *Science* **1993**, *261*, 1567−1568.
(5) Chun, J. K. M.; Bocarsly, A. B.; Cottrell, T. R.; Benziger, J. B.; Yee, J. C. *J. Am. Chem. Soc.* **1993**, *115*, 3024−3025.
(6) Fisher, D. L.; Gamboa, A.; Harper, J.; Lauerhaas, J. M.; Sailor, M. J. *Mater. Res. Soc. Symp. Proc.* **1995**, *358*, 507−518.
(7) Fisher, D. L.; Harper, J.; Sailor, M. J. *J. Am. Chem. Soc.* **1995**, *117*, 7846−7847.
(8) Lauerhaas, J. M.; Credo, G. M.; Heinrich, J. L.; Sailor, M. J. *J. Am. Chem. Soc.* **1992**, *114*, 1911−1912.
(9) Chandler-Henderson, R. R.; Sweryda-Krawiec, B.; Coffer, J. L. *J. Phys. Chem.* **1995**, *99*, 8851−8855.
(10) Kelly, M. T.; Chun, J. K. M.; Bocarsly, A. B. *Nature* **1996**, *382*, 214−215.
(11) Harper, J.; Sailor, M. J. *Anal. Chem.* **1996**, *68*, 3713−3717.
(12) Sailor, M. J.; Heinrich, J. L.; Lauerhaas, J. M. In *Semiconductor Nanoclusters: Physical, Chemical, and Catalytic Aspects*; Kamat, P. V., Meisel, D., Eds.; Elsevier Science B. V.: Amsterdam, 1997; Vol. 103, pp 209−235.
(13) Zhang, L.; Coffer, J. L.; Wang, J.; Gutsche, C. D.; Chen, J.-J.; Chyan, O. *J. Am. Chem. Soc.* **1996**, *118*, 12840−12841.
(14) Coffer, J. L. *J. Lumin.* **1996**, *70*, 343−351.
(15) Ko, M. C.; Meyer, G. J. *Chem. Mater.* **1995**, *7*, 12−14.
(16) Rehm, J. M.; McLendon, G. L.; Fauchet, P. M. *J. Am. Chem. Soc.* **1996**, *118*, 4490−4491.
(17) Ko, M. C.; Meyer, G. J. *Chem. Mater.* **1996**, *8*, 2686−2692.
(18) Lewis, N. S. *J. Electrochem. Soc.* **1984**, *131*, 2496−2503.
(19) Shriver, D. F.; Drezdzon, M. A. *The Manipulation of Air-Sensitive Compounds*, 2nd ed.; John Wiley and Sons, Inc.: New York, 1986.

S0002-7863(97)01209-2 CCC: $14.00 © 1997 American Chemical Society

pump−thaw degassed three times prior to use. All solutions were handled under dry $N_{2(g)}$ using conventional Schlenk and syringe techniques.[19]

Photoluminescence Measurements. The samples were immersed in 10 mL of toluene in a custom-made glass cell. Aliquots of a toluene solution of the molecule of interest were then introduced via microliter syringe, the solution was stirred for 20 min, and photoluminescence measurements were made *in situ*. Reversibility of quenching was checked at the end of titration by dilution of the solution with pure toluene. Steady-state photoluminescence spectra were obtained with an Acton 0.275 m monochromator, 450 nm cutoff filter, and a UV-enhanced Princeton Instruments liquid nitrogen-cooled charge coupled device (CCD) detector. The excitation source was the 435 nm emission line (filtered through two identical narrow band-pass interference filters) from an Oriel 250 W Hg arc lamp. Incident power at the sample was always below 1.25 mW/cm^2. The excitation source was blocked between photoluminescence measurements to minimize the possibility of photoinduced decomposition of the porous Si samples. Prior studies have shown that the photophysical properties of porous Si can be degraded by extended exposure to visible or ultraviolet light.[20,21]

Photoluminescence lifetimes were measured with a 0.125 m Oriel monochromator and an Oriel model 77344 photomultiplier tube (PMT) with a wavelength sensitivity range between 160 and 900 nm. The photocurrent signal from the PMT was amplified 25 times with a Stanford Research Systems SR445 fast preamplifier and collected with a Tektronix TDS 520 digital oscilloscope. The system had an instrument-limited time resolution of 200 ns. Excitation for the time-resolved measurements was provided with 435 nm light from a laser dye cell containing coumarin 450 in ethanol, pumped by a Laser Photonics model LN 300 N_2 laser. The laser provided pulses of 2 ns duration. Photoluminescence decay half-lives were derived by measuring the time at which the integrated decay curve reached half of its final value, as described in the Results and Discussion section.

The collection optic for both steady-state and time-resolved measurements consisted of a microscope objective lens focused onto a fused silica optical fiber. The other end of the fiber was coupled to either the PMT setup or the CCD, which allowed collection of both sets of data (time resolved and steady state) from the same spot on the sample.

Infrared Spectroscopic Measurements. Fourier transform infrared spectra were collected on a Nicolet Magna 550 operating in transmission mode. Spectral resolution was 4 cm^{-1}, and typically 32 interferograms were acquired per spectrum.

Results and Discussion

Preparation and Characterization of the Porous Si Samples. Four different etch procedures were used to allow preparation of porous Si samples that displayed photoluminescence intensity covering the entire visible wavelength range. Figure 1 shows representative steady-state photoluminescence spectra of the four types of samples used in this study, and Figure 2 shows plots of the half-life (the time for the integrated photoluminescence intensity to reach $^1/_2$ of its final value, see below) of the sample of porous Si samples A and B held in vacuum and immersed in pure toluene as a function of emission wavelength. As has previously been noted, the luminescence decays of porous Si are highly nonexponential and the half-life tends to increase at longer wavelengths.[15,17] The half-lives of the porous Si samples in vacuum tend to increase monotonically with increasing wavelength, while the half-lives in toluene tend to level off below a certain wavelength. The lifetime at which the decay levels off corresponds to the quenching rate of the solvent, which is relatively energy independent.[6,8] The transmission infrared spectra of all four types of samples display absorption features characteristic of surface SiH, SiH_2, and SiH_3 species at 2085, 2110, and 2140 cm^{-1}, respectively, with no detectable surface oxide absorptions (Figure 3).[22−25] Infrared spectra acquired after the quenching experiments typically display a small $\nu_{(Si-O)}$ band at 1060 cm^{-1}, indicating that some oxidation occurs during the course of the experiments. No vibrations assignable to aromatic $\nu_{(C-C)}$ or $\nu_{(C-H)}$ vibrations were observed either before or after the quenching runs.

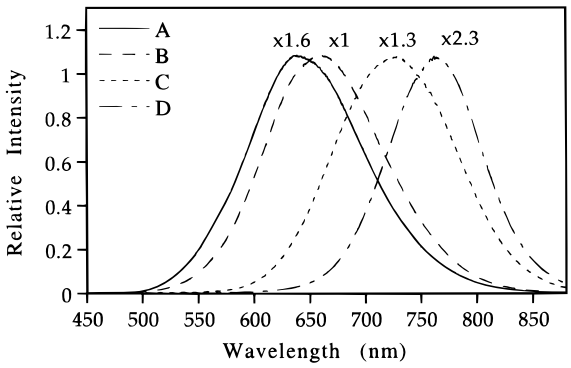

Figure 1. Steady-state photoluminescence spectra of the four types of porous Si samples used in the study. Samples A−D correspond to different sample preparation techniques as described in the text. The spectra were obtained from the samples immersed in pure (HPLC grade), deoxygenated toluene. The excitation source is the 435 nm emission line from a Hg arc lamp.

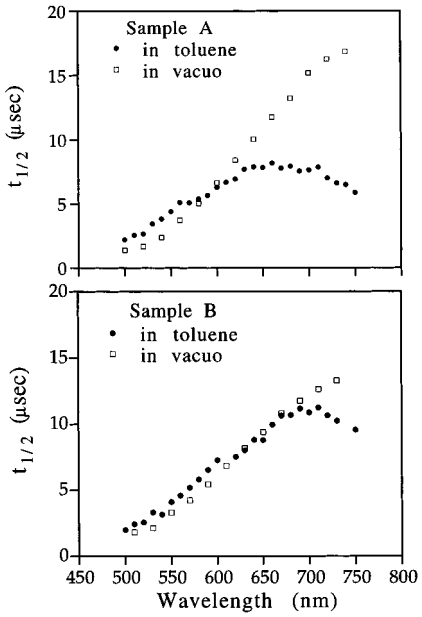

Figure 2. Half-lives of porous Si samples A (λ_{max} = 635 nm, top) and B (λ_{max} = 659 nm, bottom) used in the study measured as a function of energy. Traces marked "in toluene" (solid circles) were obtained from samples immersed in pure (HPLC grade) toluene. Traces marked "in vacuo" (open squares) were obtained from samples held at ∼10^{-3} Torr in a vacuum chamber.

Reversible Quenching Measurements and Data Analysis. Figure 4 shows the typical photoluminescence spectra observed during the course of a titration, in this case with 9,10-diphenylanthracene. There is a systematic loss of photoluminescence intensity with increasing quencher concentration. The process is reversible; in all cases, except for acridine, dilution by addition of pure solvent results in recovery of photolumi-

(20) Mauckner, G.; Thonke, K.; Sauer, R. *J. Phys.: Condens. Mater.* **1993**, *5*, L9−L14.

(21) Tischler, M. A.; Collins, R. T.; Stathis, J. H.; Tsang, J. C. *Appl. Phys. Lett.* **1992**, *60*, 639−641.

(22) Gupta, P.; Colvin, V. L.; George, S. M. *Phys. Rev. B* **1988**, *37*, 8234−8243.

(23) Dillon, A. C.; Gupta, P.; Robinson, M. B.; Bracker, A. S.; George, S. M. *J. Electron Spectrosc. Relat. Phenom.* **1990**, *54/55*, 1085−1095.

(24) Robinson, M. B.; Dillon, A. C.; Haynes, D. R.; George, S. M. *Appl. Phys. Lett.* **1992**, *61*, 1414−1416.

(25) Gupta, P.; Dillon, A. C.; Bracker, A. S.; George, S. M. *Surf. Sci.* **1991**, *245*, 360−372.

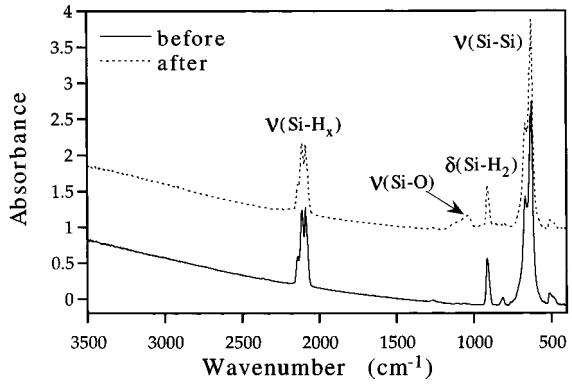

Figure 3. Transmission Fourier transform infrared spectra of a porous Si sample before (solid line) and after (dashed line) a typical quenching experiment, showing the assignment of the vibrations observed. The appearance of a band at 1060 cm^{-1} indicates that a small amount of oxidation occurs during the course of the experiments. The dashed trace has been offset by 1.0 absorbance units for clarity. The quencher used in this instance was 9,10-diphenylanthracene.

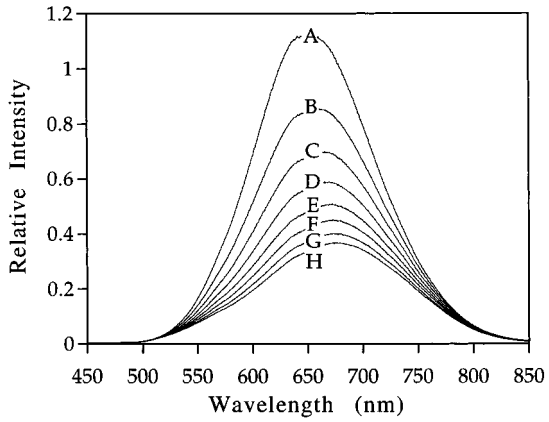

Figure 4. Steady-state emission spectra of a porous Si sample (type B) immersed in toluene upon addition of successive aliquots of solution of 9,10-diphenylanthracene in toluene. The solution concentrations of 9,10-diphenylanthracene for each trace are (A) 0.00 mM, (B) 0.393 mM, (C) 0.781 mM, (D) 1.17 mM, (E) 1.55 mM, (F) 1.92 mM, (G) 2.30 mM, and (H) 2.67 mM.

nescence to the expected intensity. The quenching data are well fit by the steady-state Stern−Volmer model.[26] Thus plots of I_o/I (measured at a given wavelength) *vs* quencher concentration yield straight lines for all of the quencher molecules studied, except as noted below (Figure 5). The slope of the Stern−Volmer plot is related to the efficiency of the quenching process via eq 1, where I_o is the photoluminescence intensity in the

$$\frac{I_o}{I} = \left(\frac{k_q}{(k_r + k_{nr})}\right)[Q] + 1 \qquad (1)$$

presence of pure toluene, I is the photoluminescence intensity in the presence of a concentration of quencher Q, k_r is the radiative rate constant, k_{nr} is the intrinsic nonradiative rate constant (not dependent on quencher), and k_q is the rate constant for quenching by molecular species. The constant k_q can also represent an equilibrium binding constant, or a product of binding constant and kinetic rate constant instead of a purely kinetic constant.[26]

The time-resolved photoluminescence decay also shows a distinct decrease in lifetime with added quencher. An example is shown for the case of 9,10-diphenylanthracene in Figure 6. As previously observed with porous silicon, the measured

(26) Turro, N. J. *Modern Molecular Photochemistry*; University Science Books: Mill Valley, CA, 1991; pp 247.

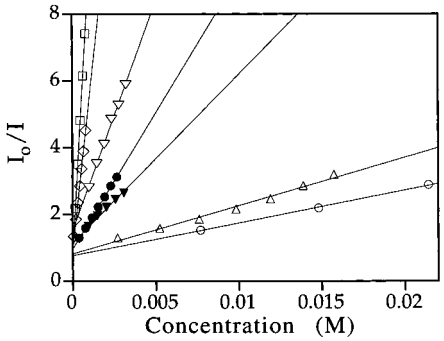

Figure 5. Steady-state Stern−Volmer plots of the quenching of photoluminescence from a type B sample of porous Si, measured at 660 nm (the maximum of emission for those samples). The reagents used for each trace (and the slopes of each trace) are (□) 9,10-dimethylanthracene (8300 M^{-1}), (◇) 9,10-dichloroanthracene (4500 M^{-1}), (▽) anthracene (1400 M^{-1}), (●) 9,10-diphenylanthracene (810 M^{-1}), (▼) 1,4-diphenyl-1,3-butadiene (470 M^{-1}), (△) 1,2-benzanthracene (140 M^{-1}), and (○) pyrene (110 M^{-1}). All solutions used degassed HPLC-grade toluene as the solvent.

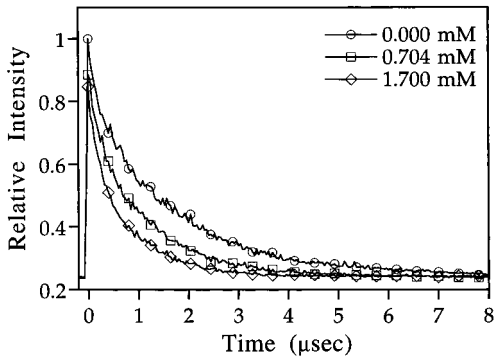

Figure 6. Time-resolved photoluminescence decays from a porous Si sample as a function of 9,10-diphenylanthracene concentration, measured at 660 nm. The decays were obtained from a type B sample held in toluene solutions of 9,10-diphenylanthracene of the indicated concentrations.

photoluminescence decays are highly nonexponential, precluding a direct comparison of the steady-state and time-resolved data.[7,15,17] Instead a value of $t_{1/2}$ (effective τ) was calculated by determining the time at which the area under the decay curve is half of the total area. The sum of intrinsic radiative and nonradiative decay rate constants for porous Si ($k_r + k_{nr}$) was assumed to be equal to the ratio (ln 2)/$t_{1/2}$ measured in pure toluene. An estimate of the rate constant for quenching, k_q, was then determined by multiplying the slope of the steady-state Stern−Volmer plot by the value of ($k_r + k_{nr}$). The value of the ratio $k_q/(k_r + k_{nr})$ taken from the steady-state data is within 1 order of magnitude of that taken from the time-resolved data for all the molecules studied, supporting the interpretation that quenching occurs by a dynamic Stern−Volmer mechanism. The values of the rate constants derived from the steady-state and time-resolved analyses are compared in Table 1.

Quenching Mechanism Attributed to Energy Transfer. We interpret the quenching mechanism as energy transfer from porous Si to the lowest triplet state of the molecular quenchers on the basis of the correlation of the logarithm of the measured values of effective k_q to the published values of the triplet energies (Figure 7). The plot of log k_q *vs* triplet energy for the molecules 9,10-dimethylanthracene, 9,10-dichloroanthracene, anthracene, 1,2-benzanthracene, and pyrene at a given value of the porous Si emission energy (660 nm) shows a monotonic decrease in quenching rate with increasing triplet energy, with a slope of approximately one decade change in rate constant for every 192 meV change in triplet energy. Thus the quenching

Table 1. Effective Quenching Rate Constants Derived from the Stern−Volmer Analyses for the Series of Molecules Studied

molecule	$10^{-7}k_q$ (M^{-1} s^{-1}) steady state[a]	time resolved[b]
9,10-dimethylanthracene	57 ± 16	140 ± 14
9,10-dichloroanthracene	34 ± 3.3	42 ± 4
anthracene	11 ± 4.7	34 ± 3
9,10-diphenylanthracene	6.3 ± 0.42	5.8 ± 0.6
1,4-diphenyl-1,3-butadiene	3.4 ± 2.1	6.8 ± 0.7
1,2-benzanthracene	0.83 ± 0.27	1.1 ± 0.1
pyrene	0.81 ± 0.16	0.52 ± 0.05

[a] Average measurement of 3−4 independent samples, measured at 660 nm. Error limits quoted are 95% confidence intervals. [b] Obtained from the plot of (ln 2)/$t_{1/2}$ *vs* quencher concentration [Q], as described in the text. Error limits quoted are estimated from instrumental reproducibility measurements.

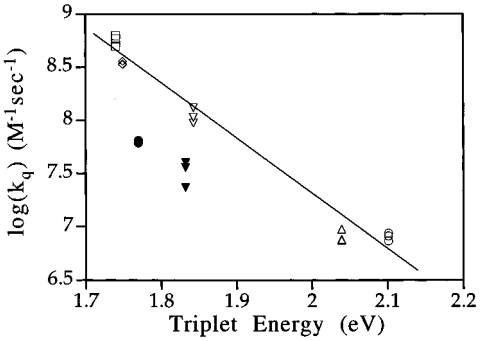

Figure 7. Plot of the logarithm of the effective quenching rate constant, derived from the Stern−Volmer analysis, versus the triplet energy of the series of energy acceptor molecules. The reagents used for each trace are (□) 9,10-dimethylanthracene, (◇) 9,10-dichloroanthracene, (▽) anthracene, (●) 9,10-diphenylanthracene, (▼) 1,4-diphenyl-1,3-butadiene, (△) 1,2-benzanthracene, and (○) pyrene. Multiple data points represent duplicate runs on different porous Si (type B) samples. Note that 9,10-diphenylanthracene and 1,4-diphenyl-1,3-butadiene are significantly below the least-squares fit line for the other molecules. This lower apparent rate is attributed to the steric bulk of 9,10-diphenylanthracene and 1,4-diphenyl-1,3-butadiene as described in the text. All plots were measured at the 660 nm emission maximum of the porous Si samples using 435 nm excitation.

process for the above series of molecules behaves as if it were in the normal Marcus (or Arrhenius) regime. The molecules 9,10-diphenylanthracene and 1,4-diphenyl-1,3-butadiene do not follow this general trend, presumably due to reduced electronic coupling of the porous Si excited state to the molecular excited state arising from steric effects (see below).

An electron-transfer quenching mechanism can be ruled out since the reduction potential of pyrene ($E° = -2.19$ V *vs* SCE) is only slightly negative of that of 9,10-dimethylanthracene ($E° = -2.15$ V *vs* SCE), while the difference in observed quenching rate constants of these two molecules is about 2 orders of magnitude. A hole-transfer mechanism can be ruled out because the ionization potentials of pyrene and anthracene are essentially the same (8.1 *vs* 8.1 eV, respectively), while the measured quenching rate constant for pyrene is 1 order of magnitude lower than that of anthracene.

Although the existence of electron or hole-transfer quenching channels is not supported by the data, it is not accurate to state that these processes are nonexistent; rather, under the current experimental conditions the energy transfer process is apparently faster than either electron or hole transfer. Rehm, McLendon, and Fauchet have reported quenching by organic and ferrocene-based molecules that have been interpreted as hole-transfer (valence band) or electron-transfer (conduction band) quenching.[16] The oxidation potentials of the molecules in the present study are more positive than the valence band quenchers of the Rehm, McLendon, and Fauchet study, and the reduction potentials of the molecules in the current study are more negative than the conduction band quenchers of the Rehm, McLendon, and Fauchet study. Thus the charge-transfer quenching rate (either electron or hole) is not expected to be large enough to be measurable in the present work.

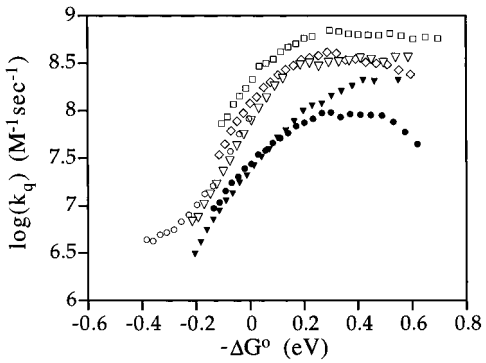

Figure 8. Correlation of the logarithm of the effective quenching rate to $-\Delta G°$, the difference between the porous Si emission energy and the triplet energy of each quencher molecule (more positive values indicate greater exoergicity). The reagents used for each trace are (□) 9,10-dimethylanthracene, (◇) 9,10-dichloroanthracene, (▽) anthracene, (●) 9,10-diphenylanthracene, (▼) 1,4-diphenyl-1,3-butadiene, and (○) pyrene.

Dependence of Quenching on Molecular Size. Even though the triplet energies of 9,10-dichloroanthracene ($E_t = 1.75$ eV) and 9,10-diphenylanthracene ($E_t = 1.77$ eV) are almost the same, the measured quenching rate constant (at 660 nm) for 9,10-diphenylanthracene is a factor of 5 smaller than that of 9,10-dichloroanthracene (Figure 7). Similarly, 1,4-diphenyl-1,3-butadiene has a triplet energy ($E_t = 1.83$ eV) close to that of anthracene ($E_t = 1.84$ eV), but the measured quenching rate constant for 1,4-diphenyl-1,3-butadiene is lower than that of anthracene by a factor of 3. These differences in rate constant exceed the experimental error of the measurements and are attributed to steric influences on the electronic coupling involved in the quenching process. All the other molecules in this study are essentially planar, but the phenyl substituents on either 1,4-diphenyl-1,3-butadiene or 9,10-diphenylanthracene are not coplanar with the rest of the molecule, making these two molecules significantly more bulky. Presumably the steric requirements of the phenyl groups do not allow these molecules to approach the Si surface as closely as the planar molecules, resulting in reduced overlap of the electronic triplet state on the molecule with the excited state in the Si nanocrystal and a lower observed quenching rate constant. Similar steric effects on triplet−triplet energy transfer rate constants have been observed previously in molecular systems.[27]

Dependence of Quenching on Porous Si Emission Energy. Figure 8 shows the energy dependence of quenching as a plot of log k_q *vs* $-\Delta G°$, where $\Delta G°$ is defined as the energy difference between the observed porous silicon emission energy (E_{em}) and the quencher molecule's triplet energy (E_t), or $E_{em} - E_t$. Since the emission bandwidth of the porous Si samples used in the present study covers a wide wavelength range, useful data were obtained with porous Si emission wavelengths between 530 and 750 nm. The data presented in Figure 8 are all from type B samples; measurements on other type samples gave comparable results. The plots show three common features, an Arrhenius-type linear region for $-\Delta G° < 0$ where the effective quenching rate constant increases with increasing driving force; a broad transition region from $-0.1 < -\Delta G° < 0.2$ eV; and a plateau region at sufficiently large driving forces

(27) Turro, N. J. *Modern Molecular Photochemistry*; University Science Books: Mill Valley, CA, 1991; pp 333.

($-\Delta G° > 0.2$ eV). In some cases a decrease in rate is observed at the highest values of the driving force. This data phenomenologically matches the classical prediction of Balzani and co-workers for highly nonadiabatic energy-transfer processes in molecular systems,[28,29] although the slope of the "linear" region is less than the theoretically predicted value of $1/(2.3RT)$. The plateaus are significantly lower than the diffusional limit, implying a very small electronic transmission coefficient and a highly nonadiabatic energy transfer process.[28] This makes sense considering that the energy donor in the present system is a nanocrystallite instead of a small solvated molecule. Pyrene and 1,2-benzanthracene displayed significant fluorescence at wavelengths below 600 nm due to direct excitation by the 435 nm excitation source; therefore the Stern−Volmer analysis for these two molecules is not accurate in the porous Si emission wavelength range < 600 nm (in Figure 8, values of $-\Delta G° > 0$ eV).

Apparently two factors are important in determining the rate of energy transfer quenching of porous Si by aromatic molecules: the first is the energy of the acceptor state and the second involves the efficiency of electronic coupling of the donor and acceptor states. We attribute the fact that the plateau regions appear at different values of log k_q to this latter factor; the electronic coupling of the molecular excited states to the porous Si excited state is highly dependent on the orientation and steric requirements of the molecule relative to the Si surface. A similar phenomenon has been noted for energy donors placed inside incarcerating molecules that separate them from the molecular acceptors.[30] In such a case the bimolecular energy-transfer rate constant can be reduced by >4 orders of magnitude when the donor and acceptor molecules are held apart by an electronically noninteracting hemicarcerand.[30] It should be noted that the plateaus with the lowest rate constant values in Figure 8 correspond to the molecules with large phenyl substituents, consistent with a weaker degree of electronic coupling with the Si nanocrystallite. It is also possible that spin selection rules are important in determining the rates of quenching, although the current set of experiments provide no insight into this possibility.

The effective quenching rate of 9,10-diphenylanthracene decreases at the highest exoergic values. A similar decrease is observed for 9,10-dichloroanthracene, although it is less pronounced. The decrease in rate constant with increasing driving force observed is suggestive of Marcus inverted region-type behavior,[31] although the relative rates involved are small and may not be significant. Interpretation of the rate data in the context of Marcus theory can provide an estimate of λ, the nuclear reorganization energy involved in the energy transfer process. The value of λ depends on the energy of bond-length changes within the reactants (the inner-sphere barrier), and the reorientation of the surrounding solvent dipoles (the outer-sphere barrier). In energy transfer, no net charge is transferred and so the solvent reorganization energy (the outer-sphere term) is expected to be fairly small. In addition, the use of the low-polarity solvent toluene in the present study ensures that the solvent reorganization energy term will be negligibly small.[32] From the maxima of the plots presented in Figure 8, a value for λ of 0.3−0.4 eV is obtained. This value is smaller than the value of the reorganization energy typically determined for electron-transfer processes, but it is in line with reorganization energies obtained for energy transfer between organic molecules.[33] For example, Closs and co-workers obtained a reorganization energy of 0.3 eV as the best fit to the Marcus equation for triplet−triplet energy transfer rates of aliphatic-bridged benzophenone/aromatic donor/acceptor molecules in benzene.[34] Similarly, Balzani and co-workers have extracted a reorganization energy of 0.12 eV for a series of aromatic triplet energy acceptors with a biacetyl donor.[30]

Acridine Quenches Porous Si Photoluminescence Irreversibly. Not all molecules studied quench photoluminescence in a reversible fashion. The heterocyclic aromatic compound acridine quenches photoluminescence from porous Si efficiently, but dilution of the solution with pure toluene does not result in recovery of photoluminescence. Infrared analysis of the porous Si surface upon removal of the solution shows significant growth of surface oxide (much greater than the increase shown in the infrared spectrum of Figure 3), but no bands that can be assigned to a surface-bound organic species. Previous workers have shown that molecules containing amine groups can quench emission from porous silicon via a Lewis acid−base interaction.[5,9,10,35] In the present work, acridine seems to strongly enhance oxide growth on the surface of the porous Si sample during the course of titration. The mechanism of oxidation is unclear, but it presumably proceeds by nucleophilic attack at a surface Si atom, activating the surface toward oxidation by traces of water present in the toluene solution. These results illustrate a limitation of using porous Si for fundamental energy transfer studies in that the acceptor molecules must be chosen with care to avoid alternate quenching or chemical reaction pathways that do not depend solely on the molecular electronic states.

Conclusions

Exposure of luminescent porous Si to toluene solutions of aromatic molecules with accessible triplet energies results in dynamic quenching of photoluminescence. The rate of quenching is dependent on the energy difference between the porous Si (donor) state and the molecular triplet (acceptor) state. The energy dependence of the rate of quenching is interpreted as arising from a highly nonadiabatic Arrhenius-type energy transfer process. There is also apparently a weak dependence of quenching rate on the size of certain substituents on the acceptor molecules. The size dependence on quenching rate is interpreted as a reduction of electronic wave function overlap between the nanocrystal and molecule as substituents increase in size.

Acknowledgment. This work was supported by the National Science Foundation (DMR-9220367), the U.S. Department of Energy, Basic Energy Sciences division, and Camille Dreyfus Teacher−Scholar and Sloan Foundation fellowships (to M.J.S.). The authors gratefully acknowledge Professor Daniel Nocera for helpful comments.

JA971209O

(28) Scandola, F.; Balzani, V. *J. Chem. Educ.* **1983**, *60*, 814−823.
(29) Balzani, V.; Bolletta, F.; Scandola, F. *J. Am. Chem. Soc.* **1980**, *102*, 2152−2163.
(30) Parola, A. J.; Pina, F.; Ferreira, E.; Maestri, M.; Balzani, V. *J. Am. Chem. Soc.* **1996**, *118*, 11610−11616.
(31) Marcus, R. A. *Angew. Chem., Int. Ed. Engl.* **1993**, *32*, 1111−1121.
(32) Kavarnos, G. J. In *Photoinduced Electron Transfer*; Mattay, J., Ed.; Springer-Verlag: New York, 1990; Vol. I, pp 21.
(33) Loeff, I.; Treinin, A.; Linschitz, H. *J. Phys. Chem.* **1992**, *96*, 5264−5272.
(34) Sigman, M. E.; Closs, G. L. *J. Phys. Chem.* **1991**, *95*, 5012−5017.
(35) Coffer, J. L.; Lilley, S. C.; Martin, R. A.; Files-Sesler, L. A. *J. Appl. Phys.* **1993**, *74*, 2094−2096.